Available online at www.sciencedirect.com
ScienceDirect
Bioorganic & Medicinal Chemistry Letters 18 (2008) 2878–2882
Bioorganic & Medicinal Chemistry Letters

Farnesyl pyrophosphate synthase enantiospecificity with a chiral risedronate analog, [6,7-dihydro-5*H*-cyclopenta[*c*]pyridin-7-yl(hydroxy)methylene]bis(phosphonic acid) (NE-10501): Synthetic, structural, and modeling studies

Sylvine Deprèle,[a] Boris A. Kashemirov,[a] James M. Hogan,[a] Frank H. Ebetino,[b] Bobby L. Barnett,[c] Artem Evdokimov[b] and Charles E. McKenna[a,*]

[a]*Department of Chemistry, University of Southern California, Los Angeles, CA 90089, USA*
[b]*Procter & Gamble Pharmaceuticals, Mason, OH 45040, USA*
[c]*Chemistry Department, University of Cincinnati, Cincinnati, OH 45221, USA*

Received 22 January 2008; revised 22 March 2008; accepted 31 March 2008
Available online 8 April 2008

Abstract—The complex formed from crystallization of human farnesyl pyrophosphate synthase (hFPPS) from a solution of racemic [6,7-dihydro-5*H*-cyclopenta[*c*]pyridin-7-yl(hydroxy)methylene]bis(phosphonic acid) (NE-10501, **8**), a chiral analog of the anti-osteoporotic drug risedronate, contained the *R* enantiomer in the enzyme active site. This enantiospecificity was assessed by computer modeling of inhibitor–active site interactions using Autodock 3, which was also evaluated for predictive ability in calculations of the known configurations of risedronate, zoledronate, and minodronate complexed in the active site of hFPPS. In comparison with these structures, the **8** complex exhibited certain differences, including the presence of only one Mg^{2+}, which could contribute to its 100-fold higher IC_{50}. An improved synthesis of **8** is described, which decreases the number of steps from 12 to 8 and increases the overall yield by 17-fold.

Bisphosphonate drugs have long been used for the treatment of bone disorders such as Paget's disease, cancer-related hypercalcemia, and postmenopausal osteoporosis,[1] but the molecular mechanisms underlying their efficacy are only recently beginning to be understood.[2,3] The first compounds in this class of drugs were introduced as stable analogs of pyrophosphate, an endogenous bone-mediating agent. Bisphosphonates (BPs) incorporate a hydrolytically inert P–C–P backbone that mimics the pyrophosphate P–O–P backbone, providing the bone mineral affinity of the natural compound, while making possible substitution at the central carbon, enabling creation of more effective drugs.

Both phosphonate groups are required for maximal affinity to bone, which is increased by the presence of an α-hydroxyl group.[4,5] The presence of a nitrogen (N-BPs) atom in a second α-substituent can confer greatly enhanced anti-osteoporotic potency, which has been associated with the inhibition of human farnesyl pyrophosphate synthase (hFPPS, EC 2.5.1.10). hFPPS catalyzes the condensation of the isoprenoid dimethylallyl pyrophosphate (DMAPP) with isopentenyl pyrophosphate (IPP).[6,7] This forms geranyl diphosphate (GPP), which then condenses with a second IPP to yield farnesyl pyrophosphate (FPP). Inhibition of hFPPS blocks prenylation of several G proteins, impairing their relocation to the cellular membrane and ultimately leading to apoptosis of the osteoclast.[2]

Recent X-ray crystallographic structures of several clinically used nitrogen-containing bisphosphonates including risedronate [(1-hydroxy-2-pyridin-3-ylethane-1,1-diyl)bis(phosphonic acid)] in complex with bacterial and human FPPS[8–10] suggest that the side-chain nitrogen of the inhibitor is positioned in the complex to form a hydrogen bond with one or more active site

Keywords: Osteoporosis; Bisphosphonates; Anti-tumor; Molecular modeling; Crystallography; Chirality.
* Corresponding author. Tel.: +1 213 740 7007; fax: +1 213 740 0930; e-mail: mckenna@usc.edu

0960-894X/$ - see front matter © 2008 Elsevier Ltd. All rights reserved.
doi:10.1016/j.bmcl.2008.03.088

residues. None of the drugs used in these studies are chiral.

To further clarify the contribution of the drug side-chain nitrogen interactions to FPPS inhibitor binding, we decided to examine by active site modeling and X-ray crystallography the relative binding of the enantiomeric forms of a chiral risedronate analog in which the rotation of the pyridine ring about the bond joining it to the linking methylene carbon is prevented by its incorporation into a rigid ring, (*R*,*S*)-[6,7-dihydro-5*H*-cyclopenta[*c*]pyridin-7-yl(hydroxy) methylene]bis(phosphonic acid) (NE-10501, **8**)[11] (Fig. 1). The racemate of this compound has an IC_{50} of 629.5 nM, thus even if one enantiomer were wholly responsible for the inhibition, its IC_{50} would exceed that of risedronate (IC_{50} = 5.7 nM)[7] by almost two orders of magnitude. Earlier work demonstrates the importance of conformational templates in examining the activity of bisphosphonates.[12]

To facilitate these and future investigations, a significantly improved synthesis of **8** was devised, which is reported here together with the results of our structural studies of the **8**-hFPPS complex.

Modeling studies: We first undertook modeling of three known hFPPS complexes of clinical bisphosphonates (minodronate, risedronate, and zoledronate) with AutoDock 3 to provide an indication of the predictive power of the program with these systems. AutoDock 3 has been used to model risedronate complexes with avian, bacterial, and recombinant human FPPS[13] and has shown[14,15] potential as a tool for the discovery of new FPPS-targeted BPs. For all three drugs, the computer model generated a consensus ensemble of bound conformers that coincided reasonably well with the experimentally determined structures (Fig. 2).[16] In these studies, IPP was not included in the model because, while IPP is required for the overall function of the enzyme in vivo, its presence is not required for the binding between N-BPs and hFPPS. The IPP binding site is fully formed only after the allylic substrate or N-BP is bound and hFPPS is triggered into a partially closed conformation.[10]

In all such docking analyses performed to date, the compared inhibitors have been different compounds, with one very recent exception where diastereomeric forms of an inhibitor were examined.[15] We therefore modeled the individual enantiomers of **8** into the active site of hFPPS (PDB ID# 1YV5) to determine whether the model would predict a significant preference for binding one over the other. For 100 docking trials with each enantiomer, the average docked energy for the *S* enantiomer was −30.86 kcal/mol over a cluster of 73 conformations, whereas the *R* enantiomer had a value of −31.33 kcal/mol in a cluster of 80 trials. As seen in Figure 3a, (*S*)-**8** docking predicts poor conformational homology with risedronate in the active site. Figure 3b shows that (*R*)-**8** demonstrates homology with a critical risedronate-binding component, the pyridinyl nitrogen. Although these absolute energies computed by Autodock 3 are considered unreliable, the relative energy difference, ~0.5 kcal/mol predicting favored binding of the *R* isomer, combined with qualitative visualization of the bound enantiomers through docking, merited experimental evaluation. Accordingly, we sought to crystallize the enzyme complex resulting from the incubation of the enzyme with racemic **8** and to determine its structure by X-ray crystallography (Fig. 4).

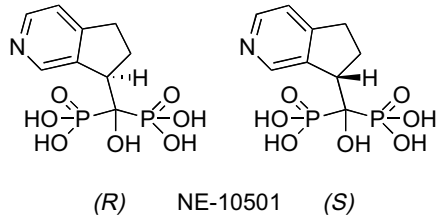

Figure 1. Structures of the enantiomers of **8**.

Synthetic studies: The synthesis of **8**, which involved the first entry into the pyrindinyl carboxylate **7** via photochemical ring contraction of 7-hydroxyisoquinoline-8-diazonium chloride **4** (Scheme 1), was previously accomplished in 12 steps with an overall yield of 0.2%.[11] Our impatience to proceed to our crystallographic studies impelled us to seek improvements to the efficiency of this route, focusing on intermediate **1**, isoquinolin-7-ol. In the original procedure, **1** was prepared by condensing 3-methoxybenzaldehyde with aminoacetaldehyde diethyl acetal in refluxing benzene, hydrogenation of the imine product to the amine with PtO_2 catalyst, tosylation, cyclodehydration by HCl in dioxane, and demethylation with BBr_3 at −78 °C. We found that these tedious multiple transformations can be replaced by an elegantly simple one-pot procedure using commercially available starting materials, in which 3-(benzyloxy)benzaldehyde is refluxed with aminoacetaldehyde dimethyl acetal until the water formed has been completely removed using a Dean–Stark trap, whereupon the condensation product is reacted in situ with trifluoroacetic acid–BF_3–Et_2O, giving **1** directly after weakly alkaline aqueous work-up, in 54% yield.[17]

Conversion of **1** to the 8-nitro derivative **2** with NO_2BF_4 in sulfolane followed the prior procedure, with the inclusion of a recrystallization step to improve purity.[18] After reduction with 10% Pd/C and acidification, the 8-amino hydrochloride salt **3** was obtained.[19]

Conversion of **3** to the diazonium chloride **4** in preparation for the subsequent photochemical ring contraction to the pyrindinyl intermediate **5** was effected with *t*-butyl nitrite as previously described,[11] but EtOH–HCl was replaced by MeOH–HCl (generated by the reaction of the dry solvent with acetyl chloride) to unify the reaction solvent, resulting in an enhanced yield.[20]

Irradiation of **4** in a high-intensity UV reactor (Rayonet) appeared to depress the yield of **5**, and we reverted to the recommended 275 W sun lamp, an original example of which was obtained from an online reseller.[21] The overall yield for the next two steps, reduction of **5** to **6** and saponification to **7** (isolated as the HCl salt), was increased about threefold by adjustments to the original procedures.[22,23]

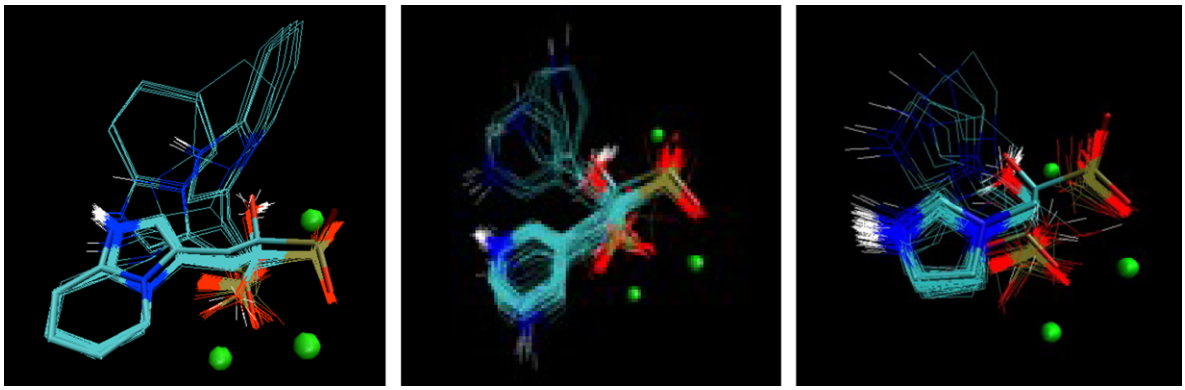

Figure 2. Docking of minodronate, risedronate, and zoledronate into the active site of hFPPS, based on their respective enzyme complex crystal structures (3B7L, 1YV5, and 2F8C). All compounds were docked as the nitrogen-protonated forms. Spheres are magnesium ions.

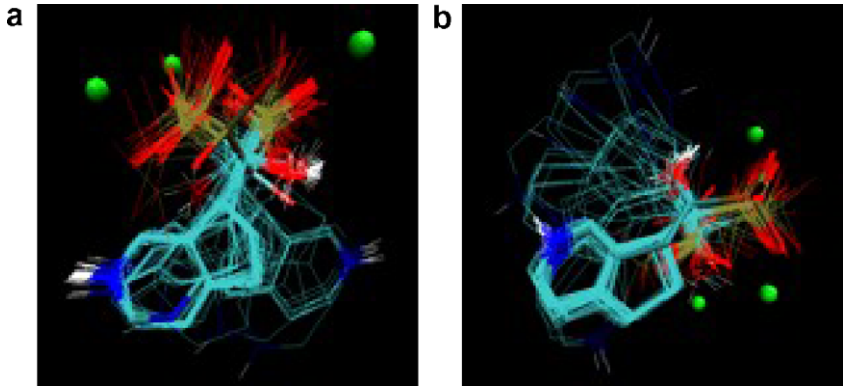

Figure 3. (a) *S*-8 docking predicts poor conformational homology with risedronate in the active site of hFPPS (1YV5). (b) *R*-8 docking gives overlap of bound risedronate's key binding element, the pyridyl nitrogen, with 80% of the calculated conformations.

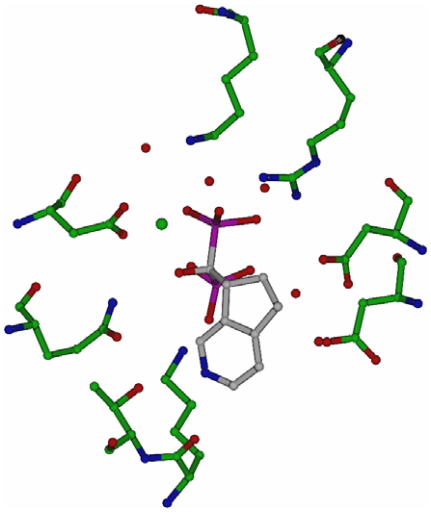

Figure 4. The crystal structure of NE-10501 in complex with hFPPS (PDB ID: 2RAH). *R* enantiomer was preferentially bound. Large spheres, Mg^{2+}; small spheres, H_2O.

The last step of the original synthesis relied upon the standard but sometimes refractory PCl_3/H_3PO_3 phosphorylation of a carboxylic acid, in this instance 7-carboxy-6,7-dihydro-5[*H*]-cyclopenta[*c*]pyridinium chloride, **7** to create the final bisphosphonate product, **8**. Although the previous report[11] demonstrated a reasonable synthetic pathway at this point, yields of only ~11% were achieved consistently. We first attempted to substitute the method of Lecouvey et al.,[24] in which 2 equiv of tris(trimethylsilyl)phosphite is reacted with a carboxylic acid or anhydride. We were unable to obtain pure 6,7-dihydro-5*H*-2-pyrinidine-7-acid hydrochloride, and therefore attempted to generate the TFA anhydride of **7**. This proved accessible in situ, but reaction with tris(trimethylsilyl) phosphite was unsuccessful. We then returned to the original reaction and using slightly different conditions,[25] succeeded in doubling the yield of the bisphosphonic acid to 23%. Substitution of toluene for the reaction solvent provided a further gain, and we finally were able to obtain pure **8** from **7** in 38% yield.[26] For the total synthesis, the overall yield is 17-fold higher than the previous method, and begins from an inexpensive, commercially available starting material.

Crystallography: Compound **8** thus prepared, was co-crystallized with hFPPS. X-ray crystallography revealed that only the *R*-isomer (PDB ID: 2RAH) was detectable in the active site of hFPPS. However, although the overall configuration of the active site complex resembles that of other inhibitor-bound FPPS structures reported to date,[27] the complex differed in that surprisingly, only a single Mg^{2+} was present. Changes in the side-chain locations of Asp 103 and Gln 171 are also apparent.

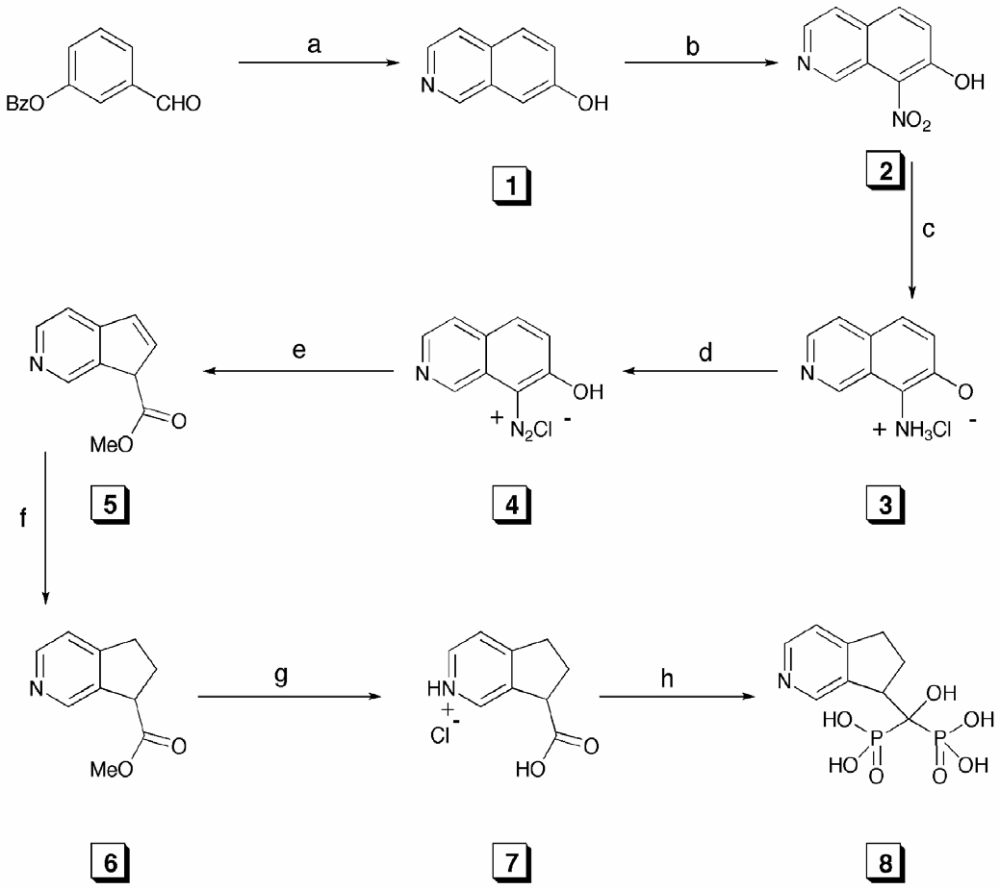

Scheme 1. Reagents and conditions: (a) i—aminoacetaldehyde dimethylacetal, toluene, 110 °C, 6 h; ii—TFA anhydride, $BF_3{\cdot}Et_2O$, <10 °C, 4 days; iii—Ether, NH_4OH to pH 9; (b) i—sulfolane, nitronium tetrafluoroborate, rt, 6 h; ii—EtOH/Et_2O (1:1); (c) i—10% Pd/C, H_2, ethanol; ii—Ether, HCl; (d) MeOH·HCl, *t*-BuONO 0 °C → rt, 4 h; (e) $NaHCO_3$, MeOH, *hv*, 0 °C, 3 h; (f) 10% Pd/C, MeOH, rt, 5 h; (g) i—NaOH, 58 °C, 4 h; ii—EtOH, HCl; (h) i—H_3PO_3, PCl_3, toluene, 110 °C, 4 h; ii—HCl, 100 °C, overnight.

Redocking of **8** into the experimentally determined active site complex still gave docking scores favoring the binding of the *R* over *S* enantiomer, although with a smaller bias (data not shown), provided that a water molecule was inserted into the position normally occupied by the Mg^{2+}, which interacts with Asp 103 and a bisphosphonate P–O oxygen (This water is present in the experimental structure but requires manual inclusion in the docking program). The presence of the rigid **8** pyridinyl ring appears to block the incorporation of this Mg^{2+} into the complex, decreasing its stability.

In summary, AutoDock 3 modeling studies were consistent with the favored conformations of risedronate, zoledronate, and minodronate in the hFPPS active site obtained by X-ray crystallography and indicated that the enzyme should preferentially bind the *R* enantiomer from a solution of racemic [6,7-dihydro-5*H*-cyclopenta[*c*]pyridin-7-yl(hydroxy)methylene] bis(phosphonic acid) **8**, for which a more efficient synthesis (8 vs 12 steps, 17× higher yield) was devised. X-ray crystallography confirmed the enantiomeric selectivity, but an unusual active site complex structure was revealed, incorporating a single Mg^{2+}. The results suggest a new structural basis to interpret the lower affinity of hFPPS for **8** relative to the three clinical drugs.

Acknowledgments

This work was supported with funding by Procter & Gamble Pharmaceuticals, Inc. Charles E. McKenna was a consultant for Procter & Gamble Pharmaceuticals, Inc., during the period of this research. Data were collected at Southeast Regional Collaborative Access Team (SER-CAT) 22-ID (or 22-BM) beamline at the Advanced Photon Source, Argonne National Laboratory. Supporting institutions may be found at www.ser-cat.org/members.html. Use of the Advanced Photon Source was supported by the U.S. Department of Energy, Office of Science, Office of Basic Energy Sciences, under Contract No. W-31-109-Eng-38.

References and notes

1. Fleisch, H.; Russell, R. G.; Francis, M. D. *Science* **1969**, *165*, 1262.
2. Green, J. R. *Oncogene* **2004**, *9*, 3.
3. Reszka, A. A.; Rodan, G. A. *Mini-Rev. Med. Chem.* **2004**, *4*, 711.
4. Fleisch, H. A.; Russell, R. G.; Bisaz, S.; Muhlbauer, R. C.; Williams, D. A. *Eur. J. Clin. Invest.* **1970**, *1*, 12.
5. Russell, R. G.; Muhlbauer, R. C.; Bisaz, S.; Williams, D. A.; Fleisch, H. *Calcif. Tissue Res.* **1970**, *6*, 183.

6. Martin, M. B.; Arnold, W.; Heath, H. T., 3rd; Urbina, J. A.; Oldfield, E. *Biochem. Biophys. Res. Commun.* **1999**, *263*, 754.
7. Dunford, J. E.; Thompson, K.; Coxon, F. P.; Luckman, S. P.; Hahn, F. M.; Poulter, C. D.; Ebetino, F. H.; Rogers, M. J. *J. Pharmacol. Exp. Ther.* **2001**, *296*, 235.
8. Hosfield, D. J.; Zhang, Y.; Dougan, D. R.; Broun, A.; Tari, L. W.; Swanson, R. V.; Finn, J. *J. Biol. Chem.* **2004**, *279*, 8526.
9. Kavanagh, K. L.; Guo, K.; Dunford, J. E.; Wu, X.; Knapp, S.; Ebetino, F. H.; Rogers, M. J.; Russell, R. G. G.; Oppermann, U. *Proc. Nat. Acad. Sci. U.S.A.* **2006**, *103*, 7829.
10. Rondeau, J.-M.; Bitsch, F.; Bourgier, E.; Geiser, M.; Hemmig, R.; Kroemer, M.; Lehmann, S.; Ramage, P.; Rieffel, S.; Strauss, A.; Green, J.; Jahnke, W. *Chem. Med. Chem.* **2006**, *1*, 267.
11. Ebetino, F. H.; Soyke, E. G., Jr.; Dansereau, S. M. *Heteroat. Chem* **2000**, *11*, 442. The structure of the title compound is depicted erroneously here.
12. Ebetino, F. H.; McOsker, J. E.; Borah, B.; Emge, T. J.; Crawford, R. J.; Berk, J. D. *Osteoporosis, Third International Symposium on Osteoporosis* **1990**, 1344.
13. Ebetino, F. H.; Rozé, C. N.; McKenna, C. E.; Barnett, B. L.; Dunford, J. E.; Russell, R. G. G.; Mieling, G. E.; Rogers, M. J. *J. Organomet. Chem.* **2005**, *690*, 2679.
14. Mao, J.; Mukherjee, S.; Zhang, Y.; Cao, R.; Sanders, J. M.; Song, Y.; Zhang, Y.; Meints, G. A.; Gao, Y. G.; Mukkamala, D.; Hudock, M. P.; Oldfield, E. *J. Am. Chem. Soc.* **2006**, *128*, 14485.
15. Hogan, J. M.; Deprèle, S.; Kashemirov, B. A.; Barnett, B.; Evdokimov, A.; Dunford, J.; Russell, R. G. G.; Ebetino, F. H.; McKenna, C. E. 234th ACS National Meeting; 2007, MEDI-073.
16. The crystal structure of risedronate in complex with hFPPS was obtained from the Protein Data Bank (PDB ID: 1YV5). This file was edited to remove water molecules and risedronate. Partial charges and solvation parameters were added using AutoDock Tools, and the magnesium ions were manually assigned a charge of +2. The grid map was calculated using AutoDock 3.0.5 (http://autodock.scripps.edu/). Ligands were constructed using Spartan '02 (Wavefunction, Inc.: Irvine, CA) and partial charges and protons were added, and torsions defined, using AutoDock Tools. Docking simulations were performed in AutoDock 3.0.5 using a Lamarckian genetic algorithm employing a rigid protein and a flexible ligand (100 independent runs per enantiomer). Calculations were carried out on a Linux operating system and the resulting structure files were analyzed using VMD 1.8.5, a visualization program (http://www.ks.uiuc.edu/Research/vmd/).
17. 3-(Benzyloxy)benzaldehyde (53.4 g, 252 mmol) and aminoacetaldehyde dimethylacetal were refluxed for 6 h in toluene (550 mL) under N_2. TFA (106 mL, 758 mmol) and $BF_3{\cdot}Et_2O$ (93 mL, 740 mmol) were added dropwise, at 10 °C. After 4 d, the product was rinsed with ether and dissolved in H_2O. The pH was increased to 9 with NH_4OH, precipitating a light brown solid, which was dried under vacuum (19.36 g, 54%). ^{1}H NMR (DMSO-d_6): δ 10.15 (s, 1H), 9.08 (s, 1H), 8.27 (d, J = 6 Hz, 1H), 7.81 (d, J = 9 Hz, 1H), 7.67 (d, J = 6 Hz, 1H), 7.32 (d, J = 9 Hz, 1H), 7.24 ppm (s, 1H).
18. NO_2BF_4 (13 g, 98 mmol) in sulfolane, was added to isoquinolin-7-ol (10 g, 69 mmol) at 0 °C. After stirring under N_2 in sulfolane (50 mL, 525 mmol) for 6 h at rt, quenching with MeOH and evaporation, the residue was treated with 100 mL of 1:1 EtOH/Et_2O. The sulfolane layer was washed with Et_2O, yielding a brown solid that was dissolved in H_2O and recrystallized with Et_2O:8-nitroisoquinolin-7-ol (9 g, 69%). ^{1}H NMR (DMSO-d_6): δ 9.27 (s, 1H), 8.60 (d, J = 6 Hz, 1H), 8.25 (d, J = 9 Hz, 1H), 8.16 (d, J = 6 Hz, 1H), and 7.74 ppm (d, J = 9 Hz, 1H).
19. 7-Hydroxyisoquinolin-8-aminium chloride (2 g, 10.5 mmol) and 10% Pd/C (0.4 g) were mixed in EtOH (50 mL) under H_2. After filtration, the solution was evaporated and the residue dissolved in MeOH (10 mL). After addition to ether (100 mL) and 4 M HCl in dioxane (7.5 mL), the product precipitated: light brown solid (1.26 g, 77%). ^{1}H NMR (DMSO-d_6): δ 9.78 (s, 1H), 8.18 (d, J = 6.7 Hz, 1H), 8.10 (d, J = 6.7 Hz, 1H), 7.65 (d, J = 8.4 Hz, 1H) and 7.29 ppm (d, J = 8.4 Hz, 1H).
20. A solution of 0.1 M methanolic HCl (31 mL) was added to 7-hydroxyisoquinolin-8-aminium chloride (0.5 g) under N_2 at 0 °C, followed by 1 mL *t*-butylnitrite. The solution was stirred for 4 h and then added to cold Et_2O (200 mL). The product after drying was a light brown solid (353 mg, 68%). ^{1}H NMR (DMSO-d_6) δ 9.09 (s, 1H), 8.52 (d, J = 5 Hz, 1H), 8.00 (d, J = 9 Hz, 1H), 7.90 (d, J = 5 Hz, 1H) and 7.00 ppm (d, J = 9 Hz, 1H).
21. A solution of 7-hydroxyisoquinoline-8-diazonium chloride (355 mg, 1.7 mmol) and sodium bicarbonate (271 mg, 3.22 mmol) in dry MeOH (500 mL), at 0 °C, was irradiated with a 275-W sun lamp for 3 h. The solvent was removed and the residue extracted with CH_2Cl_2. The extracts were evaporated: red–orange solid (225 mg, 76%). ^{1}H NMR (DMSO-d_6): δ 8.81 (s, 1H), 7.67 (d, J = 4 Hz, 1H), 7.59 (d, J = 6 Hz, 1H), 7.54 (d, J = 6 Hz, 1H), 6.39 (d, J = 4 Hz, 1H) and 3.72 ppm (s, 3H).
22. Methyl 7[*H*]-cyclopenta[*c*]pyridine-7-carboxylate (440 mg, 2.51 mmol) and 10% Pd/C (1.07 g) in MeOH were kept under H_2 for 5 h. The mixture was filtered and the solvent removed: light brown oil (311 mg, 70%). ^{1}H NMR (DMSO-d_6): δ 7.67 (s, 1H), 7.55 (d, J = 4.7 Hz, 1H), 6.50 (d, J = 4.7 Hz, 1H), 3.38 (t, J = 8 Hz, 1H), 2.85 (s, 1H), 2.11 (m, 1H) and 1.50 ppm (m, 2H).
23. Methyl 6,7-dihydro-5[*H*]-cyclopenta[*c*]pyridine-7-carboxylate (450 mg, 2.54 mmol) in 1.0 M NaOH (2.6 mmol) in MeOH (26 mL) was stirred at 58 °C for 4 h. The solvent was removed and the residue dissolved in 10 mL EtOH. The addition of 4.0 M HCl (1.25 mL) in dioxane, followed by cold Et_2O gave a solid, dried under vacuum (460 mg, 90%). ^{1}H NMR (DMSO-d_6): δ 12.04 (s, 1H), 8.75 (s, 1H), 8.63 (d, 1H), 7.81 (d, 1H), 4.28 (t, J = 7.2 Hz, 1H), 3.11 (m, 2H) and 2.32 ppm (m, 2H).
24. Lecouvey, M.; Mallard, I.; Bailly, T.; Burgada, R.; Leroux, Y. *Tetrahedron Lett.* **2001**, *42*, 8475.
25. Kieczykowski, G. R.; Jobson, R. B.; Melillo, D. G.; Reinhold, D. F.; Grenda, V. J.; Shinkai, I. *J. Org. Chem.* **1995**, *60*, 8310.
26. 7-Carboxy-6,7-dihydro-5[*H*]-cyclopenta[*c*]pyridinium chloride (140 mg, 0.7 mmol) and phosphorous acid (180.6 mg, 2.2 mmol) were stirred at 80 °C in toluene until the solids melted. PCl_3 (0.2 mL, 2.29 mmol) was added dropwise and the temperature raised to 110 °C. The mixture was stirred for 4 h and the toluene decanted. The system was refluxed in 1.0 M HCl (2 mL) overnight. Water was removed in vacuo and the black solid product was rinsed with acetone and MeOH: white solid (130 mg, 38%). ^{1}H NMR (DMSO-d_6): δ 8.39 (s, 1H), 7.85 (d, 1H), 7.24 (d, 1H), 3.54 (m, 1H), 2.75 (m, 2H) and 1.92 ppm (m, 2H) ^{31}P NMR (D_2O): δ. 17.5 (d, Jp–p = 35 Hz) and 16 ppm (d, Jp–p = 35 Hz).
27. The protein was supplemented with 10 mM $MgCl_2$ and mixed with 1 mM inhibitor. After incubation, crystallization was performed using the hanging drop method, using a 1:1 ratio of protein solution and well solution, which consisted of 0.2 M ammonium sulfate, 15% isopropanol, 15% ethylene glycol, and 0.1 M sodium acetate, at pH 4.5.